Chapter 7

Study and analysis of a two-dimensional non-conservative fractional-order aerosol transport equation

7.1 Introduction

A suspension of fine solid particles or liquid droplets, in the air or another gas is called aerosol. It Includes both particles and suspending air. The most common example of the aerosol is fog, dust and geyser steam, etc. The aerosol term is first used during the First World War to express the aero-solution. Aero is microscopic particles in the air. The hydrosol terms are developed by aerosol equivalently. Hydrosol represents the collision of the system with water as a dispersed medium. When an aerosol particle is directly introduced into the gas called primary aerosols and

The contents of this chapter have been published in **Mathematical Methods in the Applied Sciences**, (9), **42**(2019) 2939-2948.

gas-to-particle conversion is called secondary aerosols. Classification of the aerosol is defined on the basis of their physical form and how they are generated like dust, fume, mist, smoke and fog. The aerosol transport phenomenon includes the physical activities viz., convective transfer, diffusion, deposition, re-suspension, electrophoresis, gravitational settling, coagulation, condensation and evaporation.

Tiny liquid and solid particles contained in the earth's atmosphere are aerosols, which influence climate and air qualities. Aerosols include sea salt, dust, volcanic ash, burning fossil fuels produced by people as well as soot, sulfates which influence the public health. The data given by NASA [165] based on the Moderate Resolution Imaging Spectroradiometer (MODIS) shows the distribution of human pollution, natural aerosols or a mixture of both. On the basis of given data by NASA, the natural sea salts are the largest source of aerosol.

The general aerosol transport equation is given as

$$\begin{aligned}\frac{\partial q(\nu,\vec{r},t)}{\partial t} =& \nabla.[D(\nu,\vec{r},t)\nabla q(\nu,\vec{r},t)] - \nabla.[U(\nu,\vec{r},t)q(\nu,\vec{r},t)] - \frac{\partial}{\partial \nu}[I(\nu,\vec{r},t)q(\nu,\vec{r},t)] \\ &+ S(\nu,\vec{r},t) + \Big(\frac{\partial q(\nu,\vec{r},t)}{\partial t}\Big)_{coag},\end{aligned} \tag{7.1}$$

where q is the differential aerosol property (e.g., volume concentration), U is the velocity of aerosol, D diffusion coefficient, I is the rate of growth due to condensation and evaporation, S is independent source term.

Coagulation is defined for any $q(\nu,t)$, given by

$$\Big(\frac{\partial q(\nu,\vec{r},t)}{\partial t}\Big)_{coag} = \frac{1}{2}\int_0^{\nu} K(u,v-u)q(u,t)q(\nu-u,t)du - q(\nu,t)\int_0^{\infty} K(u,v)q(u,t)du, \tag{7.2}$$

where $K(u,\nu)$ is the Coagulation kernel.

Recently, many researchers are involved in the field of aerosol transportation due to its direct link to climate change. Man-made aerosols may influence the climatic changes, but natural aerosols have more influence on climatic changes. Aerosols are generally found in the emissions of sources like volcanoes, bushfires and the ocean and also formed from the unnatural sources like burning fossil fuels and sulphate emissions. Their states can be solids like smoke and sea salt, liquids like water and gases like sulphur dioxide. Aerosols reflect back the energy of the sun to space through their interactions with clouds which causes the cooling of the earth. Scientists apply radiative forcing to measure this cooling. This cooling effect by aerosols is negligible as compared to the warming effects due to greenhouse gases as a result heat of the earth is increasing day by day. Again aerosols particles sometimes have a short lifetime in the atmosphere before reaching to the earth surface and as a result contribution of these particles to cooling effect. Therefore the increase in aerosols particles in natural or artificial ways like formations of carbonic, sulphate, nitrate and organic aerosol particles is a challenging job to the scientists working in the field of atmospheric sciences. Many models on aerosol transport have been developed viz., Browner *et al.* [166] developed an aerosol model for atomic spectrometry, Darquenne and Parva [167] developed a model in one-dimension for simulation of aerosol transport and deposition in the human lung. The same authors [168] have developed a simulation of aerosol in human lung in two and three dimensions. Comer *et al.* [169] solved a model of aerosol transport in sequentially bifurcating airways. In article Soldati [170] calculated the effect of turbulence and electro-hydrodynamic flows on aerosol transport and Zhang *et al.* [171] developed a model for deposition in a human oral airway and Micro-particle transport. Rajagopal *et al.* [172] utilized numerical methods to analyze the aerosol transport problem in integral system by coupling computational fluid dynamics and aerosol dynamic equation. Vignati *et al.* [173] have developed a model of the aerosol microscopic module for large scale, in the

year 2010, a model to validate the size-resolved particle dry depositions scheme for application in aerosol transport model had been developed [174]. Many researchers have studied fractional-order differential system [136, 175, 176, 177, 178, 179] due to important applications of fractional-order model; there is plenty of scope to develop better numerical methods to find approximate solutions especially for the aerosol equation in fractional-order system.

Legendre collocation method, using operational matrix, is very much reliable as Legendre polynomials involved in it are satisfying orthogonality condition. It has got considerable attention to the researchers during handling of various problems. A truncated orthogonal series is used in the method to solve differential equations. The reason behind the approach for using the technique is that the differential equation is converted into a system of algebraic equations which simplify the problem. To the best of author's knowledge, the present model has not yet been considered by any researcher and therefore we have given our effort to solve the model under prescribed initial and boundary conditions using shifted Legendre collocation method.

In the present chapter, a drive has been taken to use the shifted Legendre polynomial approximation and an operational matrix for fractional derivatives to solve the two-dimensional time-fractional aerosol transport equation. Applying the shifted Legendre polynomial and operational matrix transform, the two-dimensional PDE is converted into a system of algebraic equations. The equations thus obtained are solved using Newton method. The main focus is concerned with the effect of particle size and also the impact of fractional-order parameter on the solution profile for different particular cases.

7.2 Solution of the problem

Consider two-dimensional fractional-order aerosol transport problem with initial and boundary conditions as

$$\frac{\partial^{\alpha} C(x,y,s,t)}{\partial t^{\alpha}} = \frac{\partial}{\partial x}\Big(D(x,y,s,t).\frac{\partial C(x,y,s,t)}{\partial x}\Big) + \frac{\partial}{\partial y}\Big(D(x,y,s,t).\frac{\partial C(x,y,s,t)}{\partial y}\Big) - \frac{\partial}{\partial x}\Big(V_1(x,y,s,t).C(x,y,s,t)\Big) - \frac{\partial}{\partial y}\Big(V_2(x,y,s,t).C(x,y,s,t)\Big) - \lambda\, C(x,y,s,t), \tag{7.3}$$

where $0 < \alpha \leq 1$,

with initial condition as

$$C(x,y,s,0) = 0, 0 \leq x \leq 1, 0 \leq y \leq 1, \tag{7.4}$$

and four boundary conditions as

$$\begin{cases} C(0,y,s,t) = C_0 = t, & \dfrac{\partial C(1,y,s,t)}{\partial x} = 0, \\ \dfrac{\partial C(x,0,s,t)}{\partial y} = 0, & \dfrac{\partial C(x,1,s,t)}{\partial y} = 0, \end{cases} \tag{7.5}$$

where $D(x,y,s,t)$ is the diffusion coefficient and $V_1(x,y,s,t), V_2(x,y,s,t)$ are velocities of aerosol in the direction of x and y. By applying shifted Legendre approximate for unknown variables and using operational matrices for derivatives taking parameters' values of the equation as $D(x,y,s,t) = 10s(x^2+y)$, $V_1(x,y,s,t) = sx$ and $V_2(x,y,s,t) = sy^2$, we get an approximation form of the equation of the considered

problem (7.3) with initial condition (7.4) as

$$\begin{aligned}&(\phi(t))^T(D^{(\alpha)})^T.U.(\phi_{m,l}(x)\otimes\phi_{m,l}(y)) - 10s(y+x^2)(\phi(t))^T.U.(D^{(2)}\otimes I).\\&(\phi_{m,l}(x)\otimes\phi_{m,l}(y)) + (\phi(t))^T.U.(I\otimes D^{(2)}).(\phi_{m,l}(x)\otimes\phi_{m,l}(y)) - 19sx(\phi(t))^T.U.\\&(D^{(1)}\otimes I).(\phi_{m,l}(x)\otimes\phi_{m,l}(y)) - s(10-y^2)(\phi(t))^T.U.(I\otimes D^{(1)}).(\phi_{m,l}(x)\otimes\phi_{m,l}(y))\\&+(s+2sy+\lambda)(\phi(t))^T.U.(\phi_{m,l}(x)\otimes\phi_{m,l}(y)) + (\phi(0))^T.U.(\phi_{m,l}(x)\otimes\phi_{m,l}(y)) = 0.\end{aligned} \tag{7.6}$$

The boundary conditions (7.5) are approximated as

$$\begin{cases}(\phi_{m,\tau}(t))^T.U.(\phi_{m,l}(0)\otimes\phi_{m,l}(y)) - t = 0,\\(\phi_{m,\tau}(t))^T.U.(D^{(1)}\otimes I).(\phi_{m,l}(1)\otimes\phi_{m,l}(y)) = 0\\(\phi_{m,\tau}(t))^T.U.(I\otimes D^{(1)}).(\phi_{m,l}(x)\otimes\phi_{m,l}(0)) = 0,\\(\phi_{m,\tau}(t))^T.U.(I\otimes D^{(1)}).(\phi_{m,l}(x)\otimes\phi_{m,l}(1)) = 0.\end{cases} \tag{7.7}$$

Equation (7.6) is collocated at the points (x_i, y_i, t_j). Equations (7.7) are collocated at the points (y_i, t_j) and (x_i, t_j), where x_i and y_i are the Legendre-Gauss-Lobatto (LGL) points of $P^l_{m-1}(x)$ and $P^l_{m-1}(y)$ respectively. $t'_j s$ are the roots of shifted Legendre polynomial $P^\tau_{n+1}(t)$. Shifted LGL grids play an important role in nodal spectral methods during the numerical solution of PDEs. After collocation equations (7.6)-(7.7) are converted into a system of linear algebraic equations. The unknown matrix U can be found from obtained linear algebraic equations which have been solved using Newton iteration method by mathematical computation. The approximate solution $C(x, y, s, t)$ can be found by substituting the value of the unknown matrix U.

7.3 Numerical results and discussion

First of all, the proposed method is validated while applying on the following fractional-order two-dimensional problem to compare the obtained results with analytical results.

$$\frac{\partial^{0.4} C(x,y,t)}{\partial t^{0.4}} = d(x,y,t)\frac{\partial^2 C(x,y,t)}{\partial x^2} + e(x,y,t)\frac{\partial^2 C(x,y,t)}{\partial y^2} + q(x,y,t),$$

$$0 < x < 1, 0 < y < 1, 0 \leq t \leq 1,$$

where $d(x,y,t) = \dfrac{2\,t^{1.6}}{\pi^2\,\Gamma 0.6}$, $e(x,y,t) = \dfrac{t^{1.6}}{12\,\pi^2 \Gamma 0.6}$, $q(x,y,t) = \dfrac{25\,t^{1.6}}{12\Gamma 0.6}(t^2+2)\sin(\pi x)\sin(\pi y)$, with $C(x,y,0) = \sin(\pi x)\sin(\pi y), C(0,y,t) = C(1,y,t) = C(x,0,t) = C(x,1,t) = 0$ whose analytical solution given by Zuang and Liu [180] is $C_{exact}(x,y,t) = (t^2+1)\sin(\pi x)\sin(\pi y)$.

The absolute error $ER_m(x,y,t)$ is defined as $ER_m(x,y,t) = |C_{exac}(x,y,t) - C(x,y,t)|$. Next we define the rate of convergence as $\mu_1 = \dfrac{ER_5(x,y,t)}{ER_3(x,y,t)}$ and $\mu_2 = \dfrac{ER_7(x,y,t)}{ER_5(x,y,t)}$ such that $\mu_1, \mu_2 \in (0,1)$. When $\mu_1 > \mu_2$, that is μ_k varies from step to step with $\mu_k \to 0$ as $k \to \infty$ then method is said to be super-linearly convergence. Therefore the error analysis exhibited through the Tables 7.1 and 7.2 clearly confirm that convergence rate of the proposed method is super-linearly as the shifted Legendre polynomials in x and y increase. Since the absolute error increases with the increase in the order of the approximation of the polynomial m, therefore our proposed method is computationally effective and it takes less time to obtain the accurate result. The error analysis depicted through Figure 7.1 clearly shows the similarity in results obtained through numerical and analytical methods. After being a justification of the accuracy and reliability of the method, the author has

motivated to use the concerned method to obtain numerical solutions of the proposed model (7.3) under the conditions given in equations (7.4) and (7.5).

The normalized mass concentration $C(x, y, s, t)/C_0$ for different particle sizes $s = 0.1, 0.2$ in the standard order system ($\alpha = 1$) are calculated for a non-conservative case ($\lambda = 1 > 0$) for a particular time $t = 0.5$, which is depicted through Figure 7.2. During computation, the shifted Legendre polynomials are approximated for $m = 7$. It is seen from the figure that the mass concentration might increase or decrease with the changes in particle size. This is physically justified as in the case of cloud processing, particles with comparatively smaller size diffuse into the droplets and trace gases to get converted to particle matter within the droplets. This increases the size of the particles and produces bimodal size distribution due to evaporation of droplets. The numerical results of the normalize mass concentration factor are shown through Figure 7.3 for $\alpha = 0.4(0.2)1$ and the non-conservative case for the size of the particle $s = 0.1$ at $t = 0.5$. It is observed that the normalized mass concentration decreases as the system approaches from fractional-order to integer-order.

The variations of normalized mass concentration with respect to x and y are shown through Figure 7.4 and Figure 7.5 for $\alpha = 1$ and $\alpha = 0.4$ respectively at $t = 0.25(0.25)1.0$. In both cases the mass concentrations increase with the increase in time. It is also seen from the figures that the normalized mass concentration difference at different time level is more for integer order system ($\alpha = 1$) as compared to fractional-order system ($\alpha = 0.4$).

Table 7.1 Maximum absolute error $ER_m(x, 0.5, 1)$ for $m = 3, 5$ and 7

x	$ER_3(x, 0.5, 1)$	$ER_5(x, 0.5, 1)$	$ER_7(x, 0.5, 1)$
0.1	0.176189	2.83193×10^{-3}	2.16603×10^{-5}
0.2	0.236381	8.04808×10^{-3}	1.08223×10^{-5}
0.3	0.235152	1.03313×10^{-2}	7.21456×10^{-5}
0.4	0.215814	1.02124×10^{-2}	1.08137×10^{-4}
0.5	0.206174	9.83092×10^{-3}	1.11683×10^{-5}
0.6	0.215814	1.02124×10^{-2}	1.01137×10^{-4}
0.7	0.235152	1.03313×10^{-2}	7.21456×10^{-5}
0.8	0.236381	8.04808×10^{-3}	1.08223×10^{-5}
0.9	0.176189	2.83193×10^{-3}	1.16603×10^{-5}

Table 7.2 Maximum absolute error $ER_m(0.5, y, 1)$ for $m = 3, 5$ and 7

y	$ER_3(0.5, y, 1)$	$ER_5(0.5, y, 1)$	$ER_7(0.5, y, 1)$
0.1	0.176189	2.71464×10^{-3}	4.41613×10^{-6}
0.2	0.236381	7.93079×10^{-3}	4.27804×10^{-5}
0.3	0.235152	1.02629×10^{-2}	1.06063×10^{-5}
0.4	0.215814	1.01929×10^{-2}	1.18282×10^{-5}
0.5	0.206174	9.83092×10^{-3}	1.11683×10^{-5}
0.6	0.215814	1.01929×10^{-2}	1.18282×10^{-5}
0.7	0.235152	1.02629×10^{-2}	1.06063×10^{-5}
0.8	0.236381	7.93079×10^{-3}	4.27804×10^{-5}
0.9	0.176189	2.71464×10^{-3}	4.41613×10^{-6}

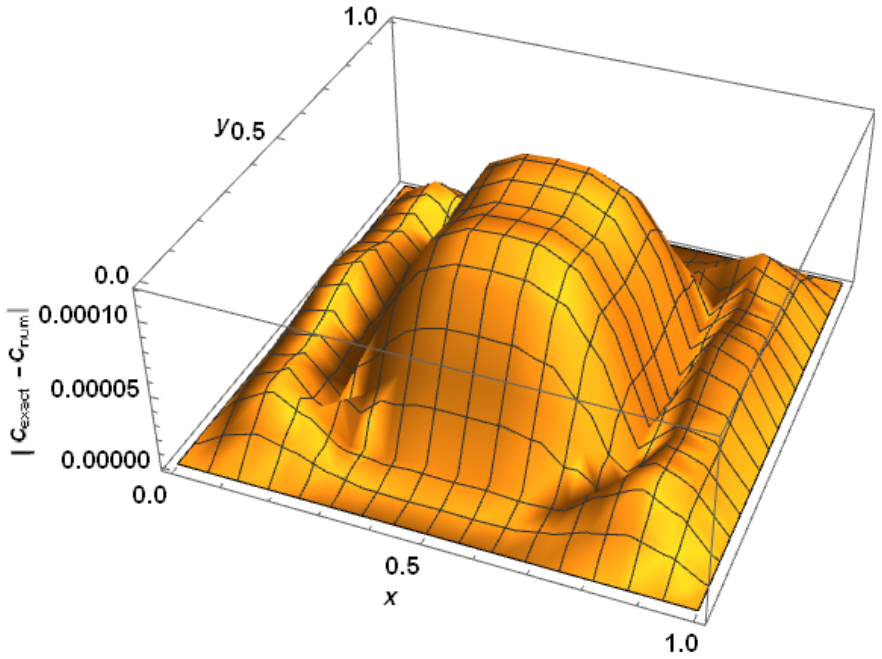

Figure 7.1: Plots of the error function $|C_{exact}(x, y, 1) - C(x, y, 1)|$ vs. x and y

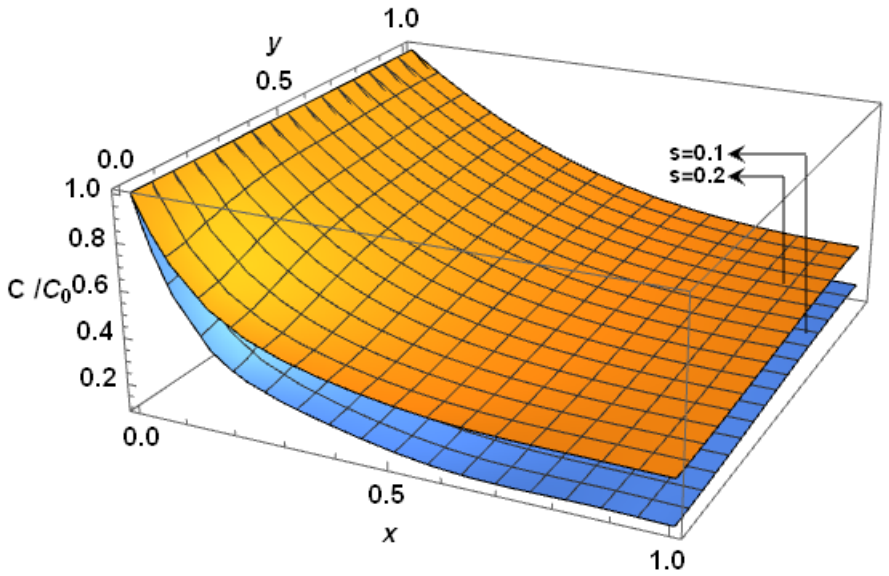

Figure 7.2: Plots of normalized mass concentration at a particular time $t = 0.5$ for different particle size $s = 0.1$ and $s = 0.2$ for $\alpha = 1$.

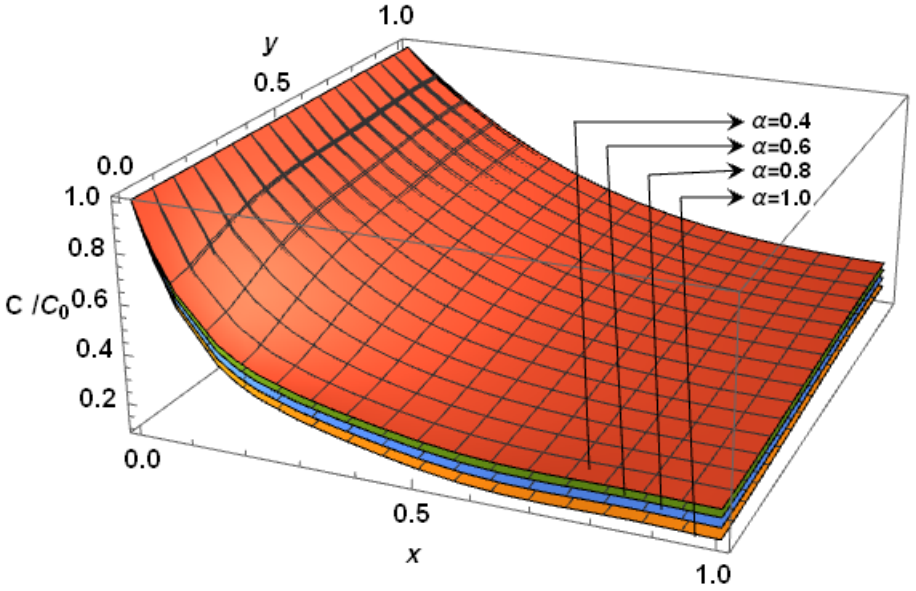

Figure 7.3: Plots of normalized mass concentration at a particular time $t = 0.5$ for different fractional time derivative $\alpha = 0.4, 0.6, 0.8$, and 1.

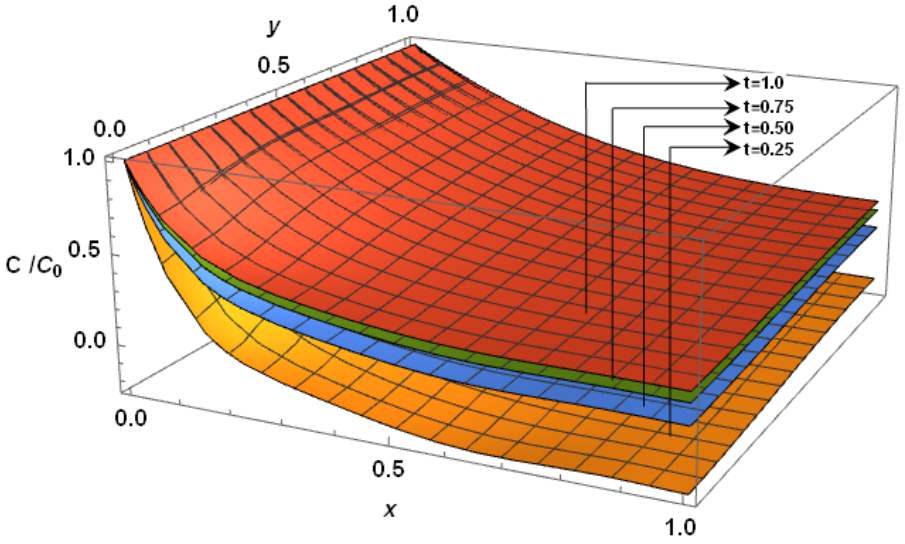

Figure 7.4: Plots of the normalized mass concentration vs. x and y for various time at particle size $s = 0.1$ for $\alpha = 1$.

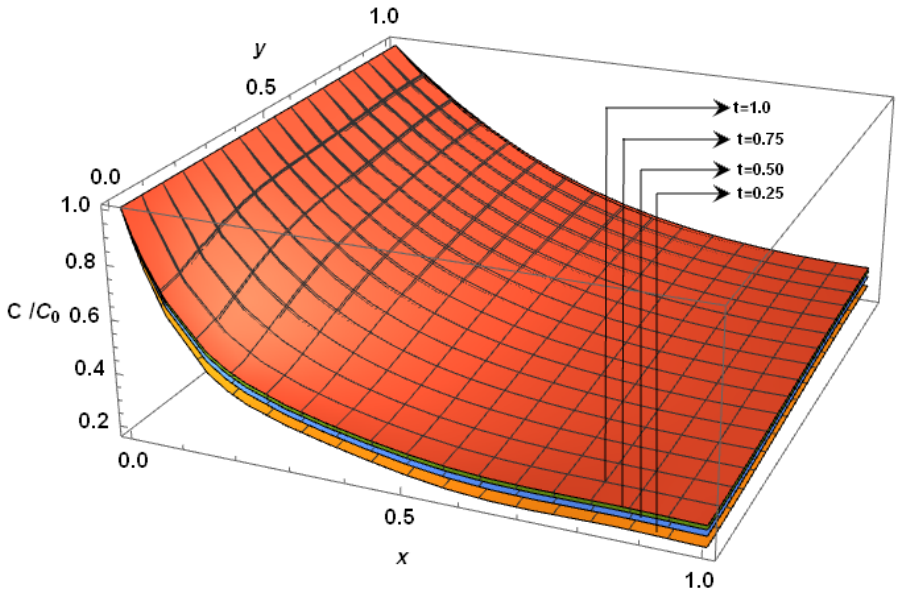

Figure 7.5: Plots of the normalized mass concentration vs. x and y for various time at particle size $s = 0.1$ for $\alpha = 0.4$.

7.4 Conclusion

The aim of this scientific contribution is to find the numerical solution of two-dimensional time fractional-order aerosol transport equation in the presence of reaction term in the finite domain using the shifted Legendre collocation method. The efficiency and effectiveness of the method are validated by comparing the results obtained by using the present method with an analytical result of the two-dimensional time fractional-order problem through error analysis. The important part of the present study is the exhibition of super-linearly convergence rate of the considered model using the proposed method. The most important point of this presentation is the graphical exhibitions of the effect of particle size on the solution profile and also variations of mass concentration when the system approaches from fractional-order

to standard order. The variation of normalized mass concentration through pictorial presentations at different time levels when the system is in fractional as well as integer orders is also an important observation of the present contribution.

****